Journal of Engineering Science and Technology
Vol. 9, No. 2 (2014) 154 - 166

DESIGN OF FILM THICKNESS INSTRUMENT FOR FIBRE POLYMER COMPOSITES TRIBOLOGICAL EXPERIMENTS

B. F. YOUSIF[1], A. AL-HADDAD[2], J. GH. ALOTAIBI[1], T. F. YUSAF[1]

[1]Faculty of Health, Engineering and Sciences, University of Southern Queensland, QLD 4350, Australia
[2]Faculty of Engineering, Universiti Teknologi Malaysia (UTM), Johor, Malaysia
*Corresponding Author: Belal.Yousif@usq.edu.au

Abstract

New technique to measure film thickness in tribological experiments is presented in the current study. The technique is based on strain gauges circuit fixed on a lever of the block on ring (BOR) machine. Conversion of strain gauge readings was made to determine the film thickness values. For testing purposes, experiments were conducted using the new machine to investigate the wear performance of glass/polyester composites. The tests were performed against aluminium counterface at different applied loads (0.5 N to 3 N) for 10 minutes sliding time under wet contact conditions. From the results, the new technique highly assisted to analysis the tribological results. The SEM showed different damage features.

Keywords: Film thickness, Tribology, Design, Composites.

1. Introduction

The endurance of machine elements such as gears, bearings and seals relies on the integrity of the lubricant film separating the contact surfaces. The thickness of a lubricant depends on the lubricant properties, the geometry of the contacted bodies and the operating conditions [1-4]. Existing techniques for lubricant-film measurement are either electrical or optical methods [5-10]. In electrical methods, the works focused on the determination of the film thickness by measuring its electrical resistance [5] and capacitance [6], or using micro-transducers [7] which founded to be more effective. However, those methods require electrical isolation of the contact elements which is be difficult task, and expensive in tribological experiments. Therefore optical methods have been recently proposed which require either that one of the contact elements is transparent or that it contains a transparent window.

Optical interferometry [8, 9] has proved successful in the measurement of elastohydrodynamic films and boundary films. In the most recent technique, the use of lasers to fluoresce a lubricant film found to be very useful method [10]. But, optical and lasers technique require a transparent environment to conduct the measurement. In practical, it is not possible to conduct tribological tests in transparent set-up especially under wet contact conditions. Moreover, reflection of the optical or lasers beams would influence the accuracy of the measurements. Nowadays, there are an interest and high demands in polymeric composites for tribological applications, e.g. bearings, bushes, etc. There are several parameters influence the wear and the frictional performance of polymeric composites such as operating parameters [11-15], fibre orientation [13], interfacial adhesion of the fibre with the matrix, and the contact condition [11, 12, 14, 15]. The contact condition (wet/dry) has an important role which controls the performance of polymeric composites [7, 10, 11, 12, 15].

In some reported works, the tribo-performance of PA, UHMWPE [15], and epoxy [12] composites improved under the wet contact condition compared to the dry conditions. The water served as a cleaner/polisher by removing wear debris from the rubbing area, and absorber for the heat generated by the frictional force. Besides, the type of lubricants used influences the performance [11]. It has been found that tribological performance of Pyrex glass and steel pins against epoxy carbon composite and Teflon discs is much better in water media compared to oil media. This was due to the low viscosity of water, where it was easy for the water to clean the rubbing surfaces compared to the oil. In previous work by corresponding author, the effect of water as lubricant on the wear and frictional performance of chopped glass fibre reinforced polyester composite was studied [13]. The generation of water film in the rubbing area was an important issue in analyzing the experimental results. This could help in understanding the wear behavior of the composite at different operating parameters. In addition, knowing the water film thickness will help to understand the surface morphology of the composites and the counterface after the experiments.

This motivates the current work on the development of new technique to measure the water film thickness during tribological experiments. The new technique is based on the use of strain gauges. The strain gauges were fixed on a flexible plastic sheet and then fixed on the lever of Block on ring (BOR) tribo-machine. Experiments were conducted to investigate the wear performance of woven glass fibre reinforced polyester composite under wet contact conditions at different applied loads.

2. Implementation of the New Technique on BOR Machine

Figure 1 shows a three dimensional view of the developed Block-on-Ring (BOR) prototype machine. The machine was designed with the aid of CATIA V5 software (Computer Aided Three dimensional Interactive Application). Technical specifications of the machine are listed in Table 1. The main components of the machine are shown in Fig. 1. The counterface (9) was made of 2011-Aluminum alloy. This type of aluminum was used due to its extensive tribological applications.

The new technique is presented in part 7, Fig. 1(a). Strain gauges were adhered on flexible plastic sheet. The plastic sheet was placed on the base of the machine

and connected to the lever as shown in Fig. 1. In this position, any strain takes place on the strain gauges can be detected. In other words, the strain gauges are able to sense any movement in the y-axis direction, which in turn they sense the gap between the rubbing surfaces (film thickness), Fig. 1(b). The strain gauges were attached on the plastic sheet using acetic silicone and covered with the same material. The strain gauges were uniaxial linear general Purposes type, made from metal material, and supplied by EMS Sdn Bhd, Malaysia. Further explanation on the strain gauges circuit is given in the following section.

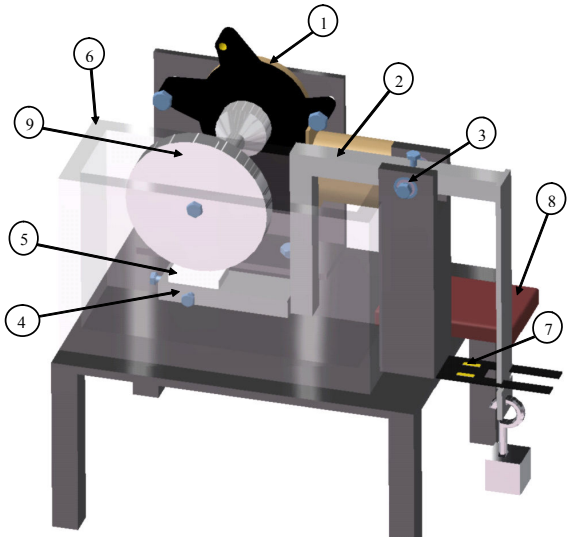

(a) Three Dimensional View of the New Machine Designed using CATIA Software.

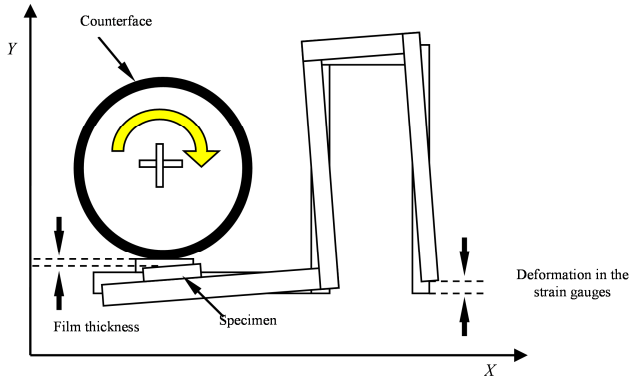

(b) Schematic Drawing Showing the Technique of Film Thickness Measurement.

Fig. 1. Block-on-Ring Machine integrated with the New Film Thickness Measurement Technique.

1 -Motor, 2- Lever, 3- Pivot, 4- Specimen holder, 5- Specimen, 6- Lubricant container, 7- Strain gauge, 8- Strain gauge sensor circuit.

Table 1. Technical Specifications of the Prototype Machine.

Motor Speed	94 rpm
Motor Type	12V DC, Torque= 9 N.m Current= 24 A.
Load	0 to 10 N
Specimen size	20 mm × 30 mm
Specimen thickness	12 mm to 18 mm

The strain gauges resistance is 120 Ohms (unstressed). This resistance changes only a fraction of a percent for the full force range of the gauge (0.01 to 1.5Ω). In order to measure the extremely small change in resistance with high accuracy, Wheatstone bridge circuit is required. If only one strain gauge (active) is used in the bridge configuration, the wire connecting the strain gauge to the circuit contributes resistances (RWIRE), in series with the strain gauge's resistance (RSG), and thus contributes to the output signal. This, of course, will be falsely interpreted by the meter as physical strain on the gauge. Moreover, an unfortunate characteristic of strain gauges is that of resistance change with changes in temperature. Thus, the Wheatstone-bridge circuit works as a thermometer just as well as it does as strain gauge as shown in Fig. 2(a).

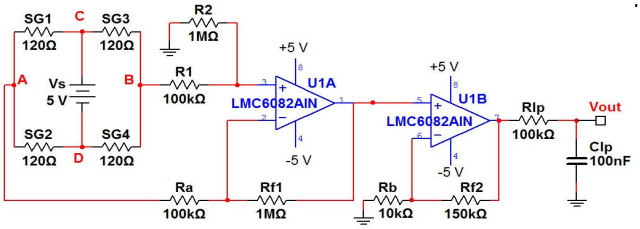

R_{SGn} = resistance of strain gauge number 1-4, R_{fn} = reference resistor, V_{CD} =Vs; the voltage of the source, R_a, R_b, R_1 and R_2 = resistors, R_{lp} and C_{lp}; resistor and capacitor of the low-pass filter.

Fig. 2(a). Schematic Diagram of the Strain Gauges Sensor Circuit.

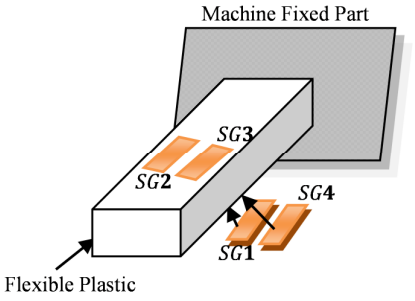

Fig. 2(b). Full-bridge Configuration of Strain Gauges.

Fig. 2. Schematic Diagram of the Strain Gauges Sensor Circuit and Full-bridge Configuration of Strain Gauges.

However, if we were to replace all the four resistors with active strain gauges as shown in Fig 2(b) by placing two upper strain gauges SG_2 and SG_3 on the plastic prototype and place the other two lower strain gauges SG_1 and SG_4 on the other side of the plastic prototype so that they are exposed to the opposite force (i.e., when the upper gauges are compressed, the lower gauges will be stretched, and vice-versa), we will have all gauges responding to strain, and the bridge will be more responsive to applied force. This utilization is known as a full-bridge. The strain gauges *SG*1 and *SG*4 have the same resistances, because they are exposed to the same strain or stress. Likewise, the resistances of the strain gauges *SG*2 and *SG*3 have the same resistances. Since $(R_{SG1} = R_{SG4})$ and$(R_{SG2} = R_{SG3})$.

$$V_{AB} = \left(\frac{R_{SG1}-R_{SG2}}{R_{SG1}-R_{SG2}}\right)(V_S) \quad (1)$$

Wire resistance doesn't impact the accuracy of the circuit as much as before, because the wires connecting all strain gauges to the bridge are approximately equal length. Therefore, the upper and lower sections of the bridge's rheostat arm contain approximately the same amount of stray resistance, and their effects tend to cancel. In addition, since all strain gauges will either increase or decrease resistance by the same proportion in response to changes in temperature, the effects of temperature change remain cancelled and the circuit will suffer minimal temperature-induced measurement error.

The full-bridge configuration is the best to use not only because it is more sensitive, but also because it is linear. With a full-bridge, the output voltage is directly proportional to applied force, with no approximation (provided that the change in resistance caused by the applied force is equal for all four strain gauges).

Since, the Wheatstone bridge output VAB is very small (in mV). Two stage of inverting operational amplifiers are connected to the bridge and the gain of the amplifiers is set to 160. The op-amp used is LMC6082 dual operational amplifiers, which is rail-to-rail op-amp. The output voltage is calculated as follows:

$$V_{out} = \left(\frac{R_{SG1}-R_{SG2}}{R_{SG1}-R_{SG2}}\right)(V_S)\,(160) \quad (2)$$

With no applied force, the plastic prototype is flat and, the resistances of all the strain gauges are equal. Hence, the bridge should be in a balanced condition and the voltmeter should register 0 volts. If the temperature changes, all gauge resistances will change by the same percentage, and the bridge's state of balance will remain unaffected. Only a differential resistance (difference of resistance between the upper and lower strain gauges) produced by physical force on the plastic prototype can alter the balance of the bridge.

An analogue 16 Hz low-pass filter is added to the output voltage of the circuit to reduce the voltage fluctuations caused by high-frequency noise. Since it is difficult to know the exact value of the input capacitances of the amplifiers, the value of the filter capacitance is experimentally adjusted so that the high frequency noise is filtered.

Conversion of strain gauge circuit reading

Conversion of strain gauge reading into film thickness was preformed to represent the film-thickness (mm) in terms of output voltage (mV), Fig. 3(a). In the process, the output voltage values were recorded using the voltmeter and the oscilloscope under different displacements of the film thickness (0-1 mm). Different known thicknesses of thin sheets are placed between the specimen and the coutnerface. For each thickness, the oscilloscope and strain gauge readings are recorded for validation and calibration purposes. The process was repeated for three times and the average of the captured data (output voltages, and film thickness) at each reading is plotted as shown in Fig. 3(b). Fitting line is generated and the displaced equation is used to convert the voltage readings to film thickness (mm) during the tribological tests.

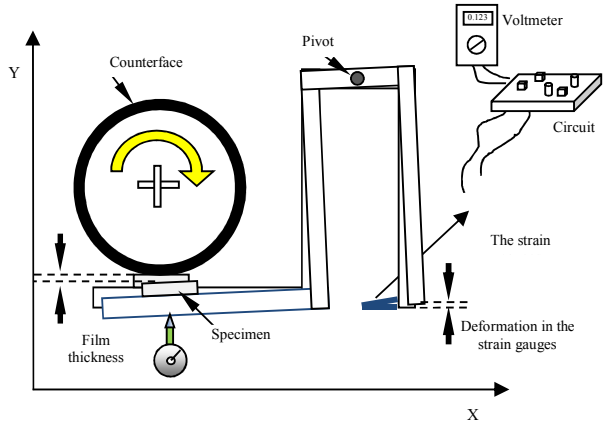

(a) Schematic Drawing Showing the Conversion of Strain Gauges Reading.

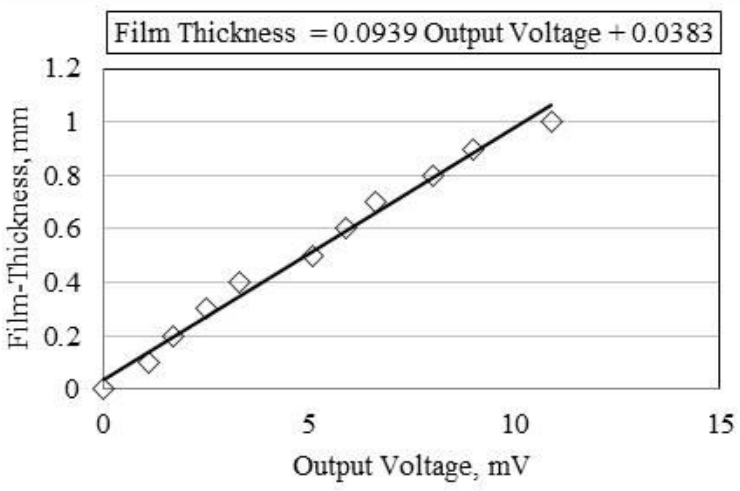

(b) Output Voltage Reading vs. Film Thickness Measurement.

Fig. 3. Conversion of Strain Gauges Readings into the Film Thickness.

3. Material Preparation and Tribological Experiments

Woven glass fabric (600 g/m^2) reinforced unsaturated polyester composite was selected material for the current experiments. A hand lay-up technique was adapted to fabricate the composite. In the fabrication process, a metal mould was coated with a thin layer of liquid polyvinyl acetate (PVA) as release agent. A paint roller soaked with polyester resin rolled over the bottom surface of the mould to make the first layer of polyester resin, followed up by a layer of the woven glass fibre mat. During the buildup of the composite block, entrapped air between the layers was squeezed out using a smooth steel roller. This process ensured that polyester resin layers were distributed uniformly over the surfaces. The process was repeated until a composite block was built up of 11 layers of woven glass fibres and 13 layers of polyester. Upper and lower layers of the block were polyester. The composite block was cured under room temperature (24^{o}C) for 24 hours. A virgin surface of the final composite material is shown in Fig. 4.

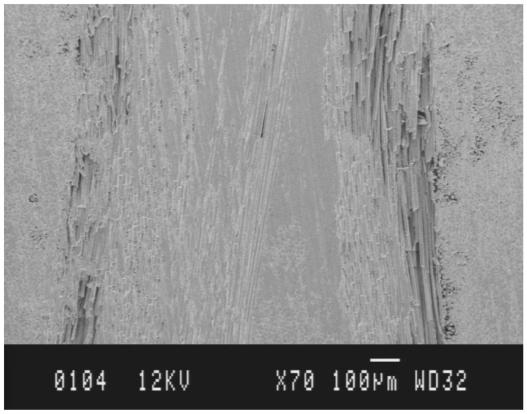

Fig. 4. Virgin Surface of the Woven Glass Fibres Reinforced Polyester Composites.

The tribological experiments were conducted using newly developed Block-on-Ring (BOR) machine, Fig. 1(a). Nowadays, several researchers focused their works on investigating the tribological behaviour of aluminium due to its superior properties compared to other metals, i.e., higher specific strength and stiffness, higher wear resistances and lower thermal expansion coefficients. The aluminium material has found use in aerospace, automotive, electronic packaging and recreational products. Therefore, the counterface material of the current prototype machine is made of 2011-Aluminum ring. Since the machine is a prototype, the aluminium material was selected for the counterface. Wet sliding tests were conducted at ambient conditions at different applied loads (0.5-3N) at rotational speed of 96 rpm for 10 minutes. Before each test, the counterface was ground and polished using an abrasive paper (G2000). Beside, the prepared specimens (20 mm × 30 mm × 15 mm) were polished against 2000 grad SiC paper to ensure an intimate line contact between the sliding face of the specimen and the counterface.

The weight loss of the specimens was determined after each test using a ±0.01 mg balance (Shimadzu AW120). Each specimen was tested at least three

times, and then the average of the weight loss (Wl) was calculated at each condition. The average of set of readings (weight loss and film thickness) associated with the maximum and minimum values are plotted against load and/or time. The standard deviation for each three test was calculated and the overall typical standard deviation of the whole set of results was found to be about 0.05-0.1 for the weight loss and 0.08-0.12 for the film thickness readings. Scanning electron microscopy SEM (JEOL, JSM 840) was used to examine the worn surface of the composite after the tests.

4. Results and Discussion

Film thickness relation vs. time and applied load, wear results, and SEM micrographs of the composite worn surface are presented in Figs. 5-7. The relation between the film thickness, sliding time, and the applied load is presented in Figs. 5(a)-(c). The results in Figs. 5(b) and (c) are the average of three readings associated with the maximum and minimum values. In Fig. 5(a), film thickness reduces when the applied load was increasing. This is clearly displayed in Fig. 5(b) which shows the average of the film thickness after 10 minutes sliding time. It seems that the higher the load is the smaller the film thickness is. In other word, applied load has very high influence on the film thickness generated during the sliding. Moreover, after 2 N applied load, the film thickness reaches the lowest values (below 0.1 mm). At this range of applied load, the composite surface starts contacting the counterface surface. In other word, wear process takes place after about 2 N applied load. This can be clarified by the wear and SEM results in the following section. On the other hand, the variation of the film thickness with the time is not remarkable.

In Fig. 5(c), steady state of film thickness can be noticed after about 30 seconds. Figure 6 displays the wear performance of the composite with the film thickness values at different applied load. The wear behaviour is presented by the weight loss determined after each test. Apparently, the figure shows that weight loss increases when the applied load was increasing, i.e., reduction in the film thickness. When the film thickness was large at lower applied load, the weight loss in the composite was almost zero. In spite of the film thickness presence at lower applied load, weight loss took place. This could be due to the shear force acted on the composite surface which was generated by the water film. In other words, it seems that wear process can take place in two mechanisms depending on the ranges of applied load.

At lower applied loads, water film can be generated and acts as shear force on the composite surface, Fig. 7(a). However, such loading is not highly damaging the composite surface compared to the high load with the absence of the water film. In other words, shear force generated in the rubbing area (between the counterface and the composite surfaces), with the absence of the water film, highly damages the composite surface, Fig. 7(b). The micrographs of the composite worn surface are presented in Fig. 8 after testing at different applied loads. At low applied load, Fig. 8(a), smoothening process took place on the composite surface. There is sign of damages on the surface. However, Fig. 6 indicates less weight loss at low applied load. The weight loss could be due to the washing of the loss asperities on the composites surface during the test. This confirms the thought that at the lower applied load, water film was generated which presents less weight loss compared to the higher applied load.

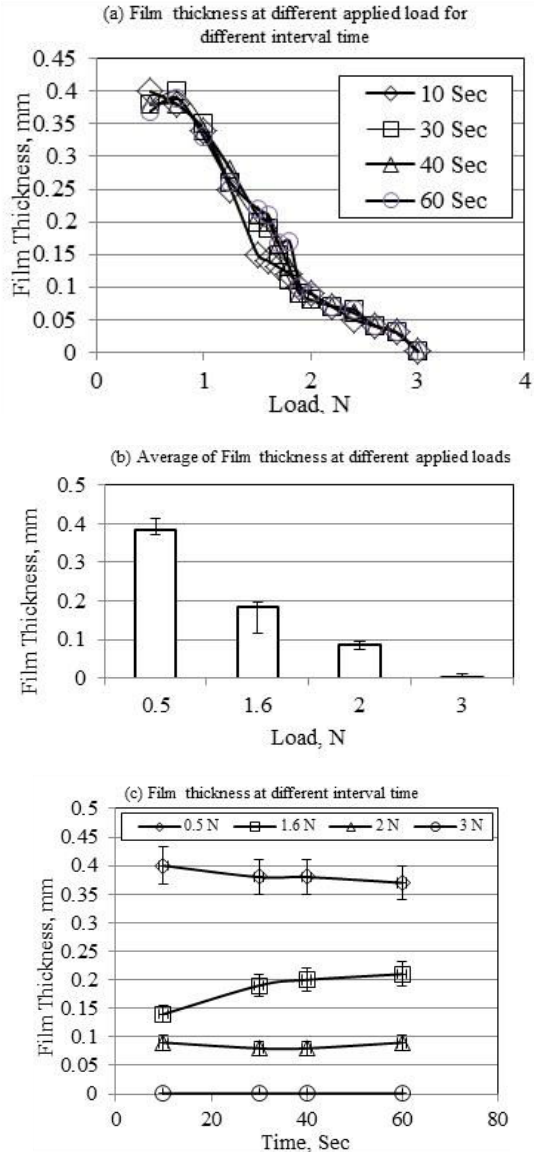

Fig. 5. The Relation between the Film Thickness, the Applied Loads and the Time.

At 2N applied load, the micrograph of the composite, Fig. 8(b) seems to be rough compared to the one shown at low applied load, Fig. 8(a). Moreover, large loss debris attached on the surface is appeared. This indicates the higher weight loss at 2 N applied load compared to the 1 N, which confirms the results presented in Fig. 6. At 2 N applied load, the water film was much lesser than the one presence at 1 N applied load (Fig. 6); this indicates a contact of asperities between the counterface and the composite surface.

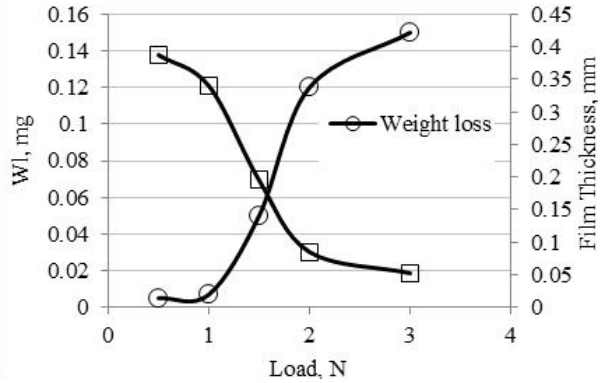

Fig. 6. The Weight Loss and the Film Thickness against Different Applied Loads.

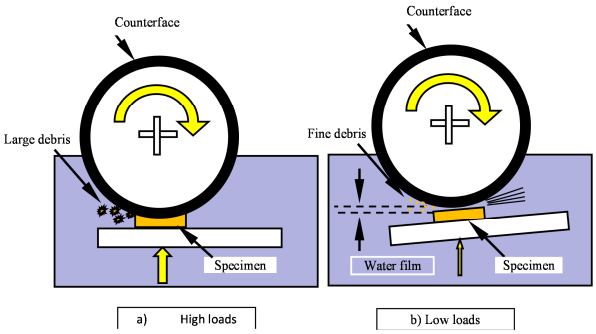

Fig. 7. Schematic Drawing Showing the Wear Process on the Composite Surface at High and Low Applied Loads.

At 3 N applied load, complete rubbing contact between the counterface and the composite surface took place as can be seen in Fig. 8(c). The micrograph in Fig. 8(c) shows that a part of the outer polyester layer was removed after the test. This indicates that the water film was absence at higher load, and removal of materials from the composite surface occurred. This is in agreement with the results presented in Fig. 5.

It has been reported that the tribological performance of PA, UHMWPE [15], epoxy [12], and polyester [13] composites enhanced under wet contact condition compared to dry. This has been due to the advantages of using water which served as a cleaner/polisher by removing wear debris from the rubbing area and assisted to reduce the heat generated by the friction. Beside the advantages of water as cleaner and/or heat absorber, it could be another reason of the lower wear rate at low applied load which is the separation of the rubbing parts due to the presence of the water film. This is confirmed in the current work when the composite was tested at low applied load. From the above, it is recommended to study the film thickness during wet adhesive experiments which will help the researcher to analysis the results. Moreover, the applied load influences the film thickness which in turn plays a main role in the application of such materials.

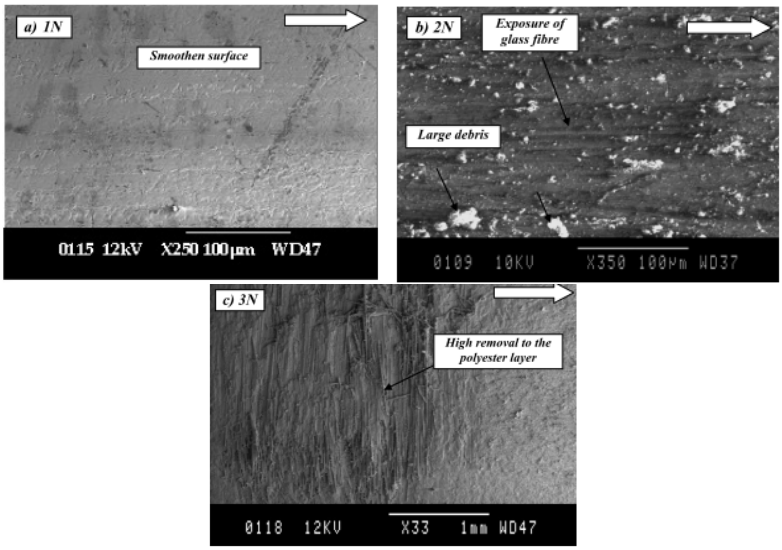

Fig. 8. The Worn Surface of the Composite after the Tests at Different Applied Loads.

New techniques have been developed for measuring film thickness in the recent year (2011), [16-18]. In [16], silicon nitride tips are fixed to the end of a triangular cantilever to sense the film thickness during the operating conditions. This technique is based on the deflection movements of the beam (lever in tribology machine) which is monitored by microprojector. The microprojector is connected to the computer to convert the captured images into film thickness readings. A calibration was needed to gain accurate results for each sample used. One of the limitations of this technique is that the accuracy of the measurement is not good at low uniformity of the lubricant. In addition, it has three steps of calibration (deflection signal, microprojectos signal, and film thickness) to gain the required thickness measurement. In the current technique, there is one conversion step which is the strain gauges reading into film thickness. This could reduce the error in readings compared to the previous technique in [16]. In other works [17, 18], an optical test apparatus was used to measure the film thickness. The main limitation of this technique is the counterpart should be glass which allows the xenon flash lamp to trigger the film thickness. In the current adopted technique, all types of tribological materials can be used which give more advantages to it compared to the optical technique.

5. Conclusion

It can be concluded that the new technique is capable to measure film thickness during wet adhesive tests. The experiments revealed few points which can be summarized as follows:

- The higher the applied load the smaller the film thickness is.
- The weight loss increases when the applied load increase. This is due to two reasons. Firstly, complete contact between the rubbing surfaces takes place at

higher applied loads. Secondly, high pressure in the rubbing area increase the shear force leading to higher removal of materials form the softer part in contact (composite surface).

- The observation on the worn surface showed that high applied load causes higher damages on the composite surface due to the above reasons. Detachments of a part of the outer polyester layer were worn away.
- The technique of film thickness measurement during the tribological experiments is highly assisted to analyze the results, especially, at lower range of applied loads.
- The new technique is found to be more reliable and easier than the previous techniques such as mechanical and optical which required either high skill of calibration and/or transparent counterface.
- It is recommended to adopt the current technique on other tribological experimental rigs and more works considering different rotational speeds is important. This due to the fact that higher rotational speed influences the film thickness.

References

1. Hwang, Y.; Lee, C.; Choi, Y.; Cheong, S.; Kim, D.; Lee, K.; Lee, J.; and Kim, S.H. (2011). Effect of the size and morphology of particles dispersed in nano-oil on friction performance between rotating discs. *Journal of Mechanical Science and Technology*, 25(11), 2853-2857
2. Singh, R.A.; Kim, H.J.; Kim, J.; Sungwook, Y.; Jeong, H.E.; Suh, K.Y.; and Yoon, E.-S. (2007). A biomimetic approach for effective reduction in micro-scale friction by direct replication of topography of natural water-repellent surfaces. *Journal of Mechanical Science and Technology*, 21(4), 624-629
3. Sasaki, S. (2010). Environmentally friendly tribology (Eco-tribology). *Journal of Mechanical Science and Technology*, 24(1), 67-71
4. Glovnea, R.P.; Forrest, A.K.; Olver, A.V.; and Spikes, H.A. (2003). Measurement of sub-nanometer lubricant films using ultra-thin film interferometry. *Tribology Letters*, 15(3), 217-230.
5. El-Sisi, S.I.; and Shawki, G.S.A. (1960). Measurement of oil-film thickness between disks by electrical conductivity. *Journal of Basic Engineering*, 82(1), 12-16.
6. Astridge, D.G.; and Longfield, M.D. (1967). Capacitance measurement and oil film thickness in a large radius disc and ring machine. *Proceedings of the Institution of Mechanical Engineers*, 182(3), 89-96.
7. Hamilton, G.M.; and Moore, S.L. (1967). A modified gauge for investigating an elastohydrodynamic contact. *Proceedings of the Institution of Mechanical Engineers*, 182(3A), 251.
8. Cameron, A.; and Gohar, R. (1966). Theoretical and experimental studies of the oil film in lubricated point contact. *Proceedings of the Royal Society A*, 291, 520-536.

9. Johnston, G.J.; Wayte, R.; and Spikes, H.A. (1991). The measurement and study of very thin lubricant films in concentrated contacts. *Tribology Transactions*, 34(2), 187-194.
10. Richardson, D.A.; and Borman, G.L. (1991). Using fibre optics and laser fluorescence for measuring thin oil films with applications to engines. *SAE Technical Paper Serial No.* 912388.
11. Borruto, A.; Crivellone, G.; and Marani, F. (1998). Influence of surface wettability on friction and wear tests. *Wear*, 222(1), 57-65.
12. Wu, J.; and Cheng, X.H. (2006). The tribological properties of Kevlar pulp reinforced epoxy composites under dry sliding and water lubricated condition. *Wear*, 261(11-12), 1293-1297.
13. Yousif, B.F.; and El-Tayeb, N.S.M. (2008). Wear and friction characteristics of CGRP composite under wet contact condition using two different test techniques. *Wear*, 265(5-6), 856-864.
14. Yousif, B.F.; and El-Tayeb, N.S.M. (2008). Adhesive wear performance of T-OPRP and UT-OPRP using BOR technique. *Tribology letters*, 32(3), 199-208.
15. Liu, C.Z.; Wu, J.Q.; Li, J.Q.; Ren, L.Q.; Tong, J.; and Arnell, A.D. (2006). Tribological behaviours of PA/UHMWPE blend under dry and lubricating condition. *Wear*, 260(1-2), 109-115.
16. Lee, H.; and Bhushan, B. (2011). Role of surface roughness and lubricant film thickness in nanolubrication of sliding components in adaptive optics. *Journal of Colloid and Interface Science*, 353(2), 574-581.
17. Vrbka, M.; Křupka, I.; Svoboda, P.; Šperka, P.; Návrat, T.; Hartl, M.; and Nohava, J. (2011). Effect of shot peening on rolling contact fatigue and lubricant film thickness within mixed lubricated non-conformal rolling/sliding contacts. *Tribology International*, 44(12), 1726-1735.
18. Mavraki, A.; and Cann P.M. (2011). Lubricating film thickness measurements with bovine serum. *Tribology International*, 44(5), 550-556.